Magnetic domain reversal in ultrathin Co(001) films probed by giant magnetoresistance measurements

S. P. Li, A. Samad, W. S. Lew, Y. B. Xu, and J. A. C. Bland*
Cavendish Laboratory, University of Cambridge, Madingley Road, Cambridge CB3 0HE, United Kingdom
(Received 3 August 1999)

The magnetic domain reversal behavior in an ultrathin Co film with in-plane anisotropy that forms part of a spin-valve structure has been investigated by giant magnetoresistance and magneto-optical Kerr effect measurements. We demonstrate that minor loops can be used to obtain detailed information on the field-dependent domain process. 90° domain boundaries are found to be strongly dominant over 180° walls in the demagnetized state, but the magnetization reversal process is controlled by 180° domain-wall motion. The 180° walls are found to undergo multiple jumps mainly due to domain-wall pinning associated with interface roughness.

I. INTRODUCTION

Recently, there has been great interest in developing experimental methods to investigate the domain structure and its dynamics in ultrathin magnetic films.[1-3] There are a number of techniques that give direct information about the domain structure, for example, transmission electron microscopy[4] (TEM), scanning electron microscopy with polarization analysis[5] (SEMPA), Kerr effect, magnetic birefringence, magneto-optical gradient effect,[6] magnetic force microscopy[7,8] (MFM), the magneto-optical indicator film[3] (MOIF) technique, etc. While these direct methods yield images of the magnetic domain structure, indirect methods based on, e.g., resistance measurements can be more convenient under certain circumstances (in high fields, very low temperatures, etc).

In this paper we use the giant magnetoresistance (GMR) effect in a spin-valve sample to detect the domain structure and magnetization-reversal processes in a ferromagnetic fcc cobalt film. As is well known, the GMR amplitude is proportional to $\cos \theta$ in a spin-valve structure, where θ is the angle between the magnetization direction in adjacent magnetic layers. The relative orientation of the magnetic moments in the film under investigation can therefore be estimated by measuring the GMR amplitude. Co is an important element widely used in spin-valve sensors,[9] and there is continuing intense interest in the domain structure and reversal behavior in ultrathin films. While many recent investigations have focused on the magnetization-reversal process of ultrathin Co films with perpendicular anisotropy,[1,10] there is currently a lack of information concerning the magnetic domain and reversal behavior in fcc Co films with in-plane anisotropy. In the present work, an epitaxial Cu/Co/Cu/FeNi/Cu spin-valve structure was grown in order to investigate the magnetic domain and reversal behavior in the fcc 40-Å Co layer.

II. EXPERIMENT AND RESULTS

We have grown an epitaxial spin-valve structure, with nominal composition Si(001)/Cu(700 Å)/Co(40 Å)/Cu(60 Å)/FeNi(60 Å)/Cu(60 Å). The sample was grown on an HF-passivated Si(001) surface at ambient temperature by molecular beam epitaxy (MBE) under ultrahigh vacuum conditions with a base pressure of $\sim 3 \times 10^{-10}$ mbar. Prior to the deposition of the magnetic materials, an epitaxial Cu(001) layer was deposited on Si(001) as a seed layer by using a Knudsen cell with a typical evaporation rate of ~ 5 Å/min. Since the lattice mismatch for the Cu[100]∥Si[110] is $\sim 6\%$, good epitaxy can be obtained on the HF-etched Si(001) substrate. The 700-Å Cu thickness was chosen to be large enough to improve the epitaxy. FeNi and Co layers were deposited on the Cu(001) surface using electron-beam evaporation, and the typical evaporation rate was ~ 1 Å/min. The pressure increased to $\sim 6 \times 10^{-10}$ mbar while FeNi and Co were being deposited and to $\sim 3 \times 10^{-9}$ mbar during Cu deposition. The deposition rates were calibrated using a quartz microbalance, which has an accuracy of $\sim \pm 10\%$. Epitaxial growth was confirmed using *in situ* reflection high-energy electron diffraction (RHEED). The images obtained showed that the FeNi and Co layers grew epitaxially in the (001) orientation, where the fcc Co[110] direction corresponds to the Si[100] direction (Fig. 1). GMR measurements were carried out using the standard four-point geometry. Hysteresis curves were measured using the longitudinal magneto-optical Kerr effect (MOKE). Each of the GMR and MOKE loops was measured by applying different field amplitudes. Before starting each measurement the sample was first saturated by applying a ''positive'' field of 1800 Oe along the Co[110] easy axis (i.e., our measurement direction). In order to investigate the demagnetized state of the Co film, the sample was dc-demagnetized and its magnetoresistance (MR) was measured under small applied field amplitudes (-25–$+25$ Oe).

Figure 2 shows the GMR loops obtained under different external field amplitudes after first saturating along the easy [110] axis. It is clear that loop 1 is a typical minor MR loop that is related to the magnetic switching of the FeNi layer, whereas the Co layer magnetization is strongly pinned in the initial direction. Its maximum and minimum resistance values correspond to the antiparallel and parallel configuration of the two magnetic layers, respectively. When the applied field amplitude is increased, the form of the GMR loop
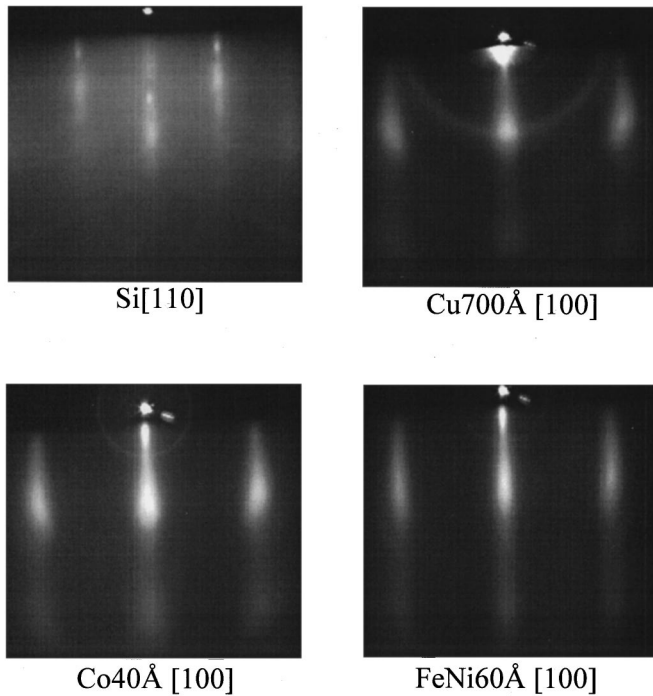
FIG. 1. RHEED images of the Si substrate, Cu buffer layer, and magnetic Co and FeNi layers.

changes, as in loop 2. This relates to magnetic switching in the Co layer. For clarity we draw schematically such a GMR loop in Fig. 2(b). Starting from point A, where the magnetization of both magnetic layers is parallel, the field is reduced to a negative value at B, whereupon the magnetization of the FeNi layer switches and becomes antiparallel to the Co layer's magnetization at C. At point D magnetic domains are formed (this is the point at which the reversal process begins) in the Co layer. Since the magnetization in both the FeNi and Co layers is not completely antiparallel (see point E), the GMR value is reduced with respect to the value at C and D. At position F the magnetization of the FeNi layer switches parallel to the applied field, whereas the magnetic configuration of the Co layer remains as before. At point H the Co layer becomes fully single domain again. A similar process occurs for loops 3 and 4, but the fraction of the magnetization in the Co layer that switches increases with increasing external field amplitude. When the field amplitude is large enough the magnetization of the Co layer can fully switch and a typical GMR loop is obtained.

In order to support the results obtained from GMR we have measured longitudinal MOKE loops for the same process, the results of which are shown in Fig. 3. From Fig. 3 we find the same magnetization reversal process as described above: When the field amplitude is relatively small there is a single switch only that is due to the FeNi layer reversal (loop 1). By increasing the field amplitude (loops 2 and 3) a second switch appears, caused by partial switching of the Co layer, and its intensity increases with field amplitude until the saturation field of the Co is reached (loop 4). Here we can see another advantage of using a spin-valve structure: Although the Kerr intensity is expressed as an arbitrary unit, we can make a relative comparison of the fraction of the Co layer magnetization switching to the intensity of the FeNi switch, which is approximately constant for each loop. Fig-
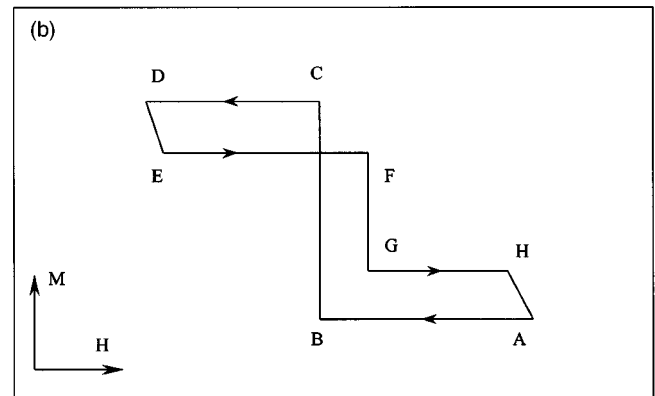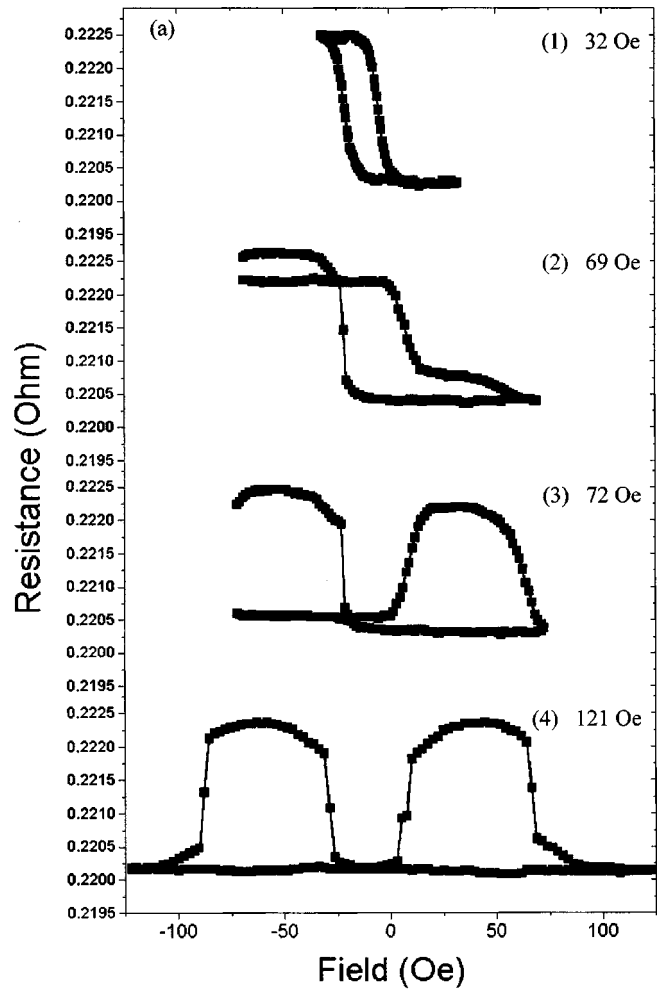

FIG. 2. (a) The GMR loops measured along the Co[110] direction for different field amplitudes after first saturating along this direction and (b) a schematic for the loop.

ure 4 shows the MR loop for small field amplitudes (±25 Oe) after the demagnetization process [Fig. 4(a)] and a GMR loop measured at higher field (±580 Oe) [Fig. 4(b)]. The difference in the observed GMR values at equivalent fields for the data of Figs. 2 and 4(b) is due to the different "four-point" measurement systems used in each case. From Fig. 4 we can see that the change in the MR [Fig. 4(a)] is much smaller than the change seen in Fig. 4(b). In Fig. 4(a) the relative alignment of the layers does not fully switch and so only the anisotropic magnetoresistance (AMR) in the FeNi layer contributes significantly to the MR loop.
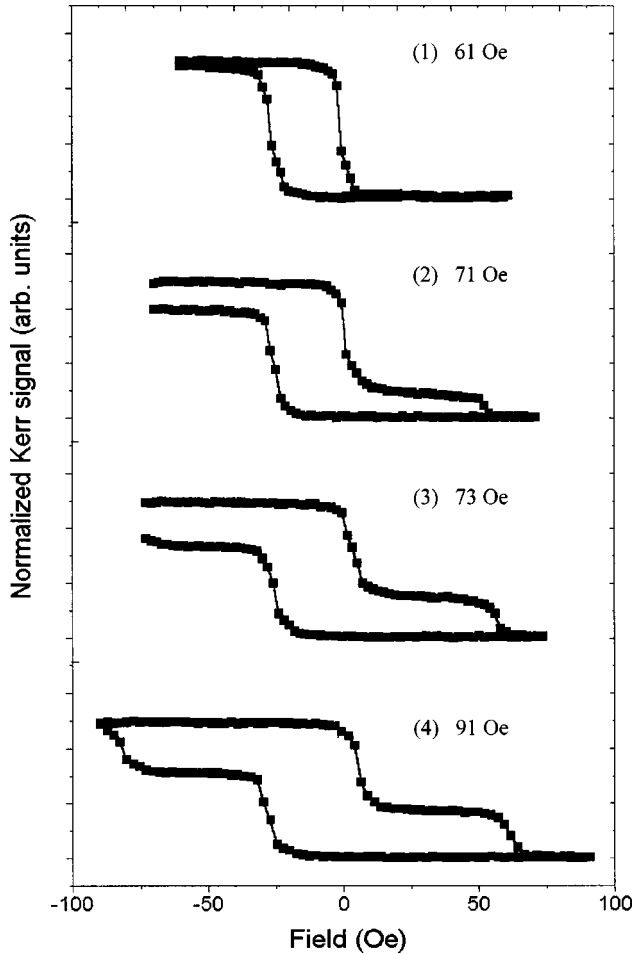
FIG. 3. Longitudinal MOKE loops measured along the Co[110] direction with different field amplitudes after first saturating along this direction.

FIG. 4. The magnetoresistance measured for small field amplitudes (±25 Oe) (a) after demagnetization and (b) a GMR loop measured at ±580 Oe.

III. DISCUSSION

A. The 90° domain wall in the demagnetized Co film

In the demagnetized state the magnetic domain walls in the fcc Co film should be mainly 90° or 180° walls due to the cubic anisotropy.[11] While we certainly cannot rule out the existence of 360° walls completely, we believe the number of such walls must be small and their contribution can therefore be neglected. We shall assume that the domain boundaries are 90° walls and the magnetization directions are equally distributed along the four easy directions $\langle 110 \rangle$. We consider a Co/Cu/FeNi spin valve in which the Co layer is demagnetized while the FeNi is saturated along the easy axis of fcc Co. The resistance of a small area including four Co domains is determined by three magnetic configurations: parallel, antiparallel, and perpendicular denoted by $\rho_{\uparrow\uparrow}$, $\rho_{\uparrow\downarrow}$, and $\rho_{\perp}$ [see Fig. 5(a)]. Assuming the effective-circuit scheme of Fig. 5(a), the measured resistance can be approximately expressed as

$$R = \frac{R_{\uparrow\uparrow}^2 + R_{\uparrow\uparrow}R_{\uparrow\downarrow}}{3R_{\uparrow\uparrow} + R_{\uparrow\downarrow}} + \frac{R_{\uparrow\uparrow}R_{\uparrow\downarrow} + R_{\uparrow\downarrow}^2}{R_{\uparrow\uparrow} + 3R_{\uparrow\downarrow}}. \qquad (1)$$

$R_{\uparrow\uparrow}$ and $R_{\uparrow\downarrow}$ represent the measured resistance when the magnetic moment in the FeNi and Co layers are parallel and
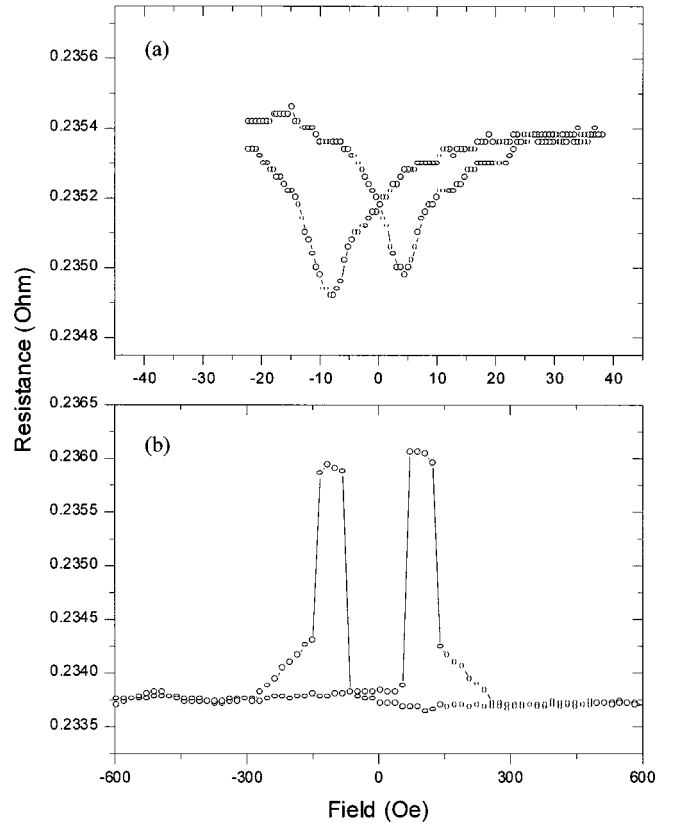
antiparallel, respectively, the values of which are taken from the GMR loop in Fig. 4(b) (i.e., the maximum and the minimum). With $R_{\uparrow\downarrow} \sim 0.2360\,\Omega$, $R_{\uparrow\uparrow} \sim 0.2338\,\Omega$, so the total resistance $R \sim 0.2349\,\Omega$, which agrees well with the experimentally observed values [Fig. 4(a)]. This indicates that in our Co film 90° boundaries are strongly dominant over 180° walls, in agreement with the result by SEMPA.[11] The possibility that 180° domain walls are distributed equally along the four axes is unlikely for several reasons. If 180° domain
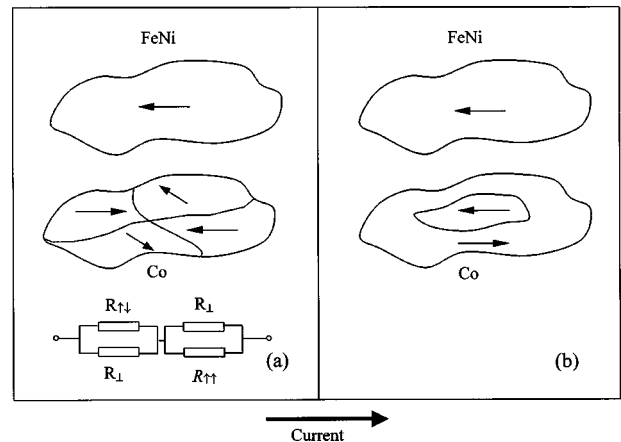

FIG. 5. Schematic of the GMR configuration assuming a flux closure domain structure in the representative area. (a) Co layer in the demagnetized state. (b) Magnetization-reversal process in a saturated Co layer.
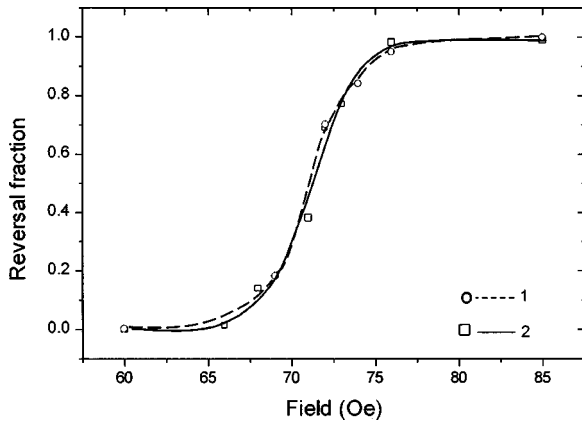
FIG. 6. The relationship between the reversal fraction k and field amplitude. Curve 1—prediction based on a model assuming 180° domain-wall motion (see text). Curve 2—experimental result from MOKE measurements.

walls were distributed equally along the four easy axes, they would give rise to 90° domain walls where they intersect. Also, the formation of a 90° wall is more favorable from an energetic point of view since $E(180°)=2E(90°)$.[11] In the absence of a strong uniaxial anisotropy, the dominant cubic anisotropy favors the formation of 90° walls.

B. 180° domain-wall motion in the reversal process of Co film

From the GMR loops shown in Fig. 2(a) we can obtain two important parameters. (i) The height of the curve EF [Fig. 2(b)] changes continuously with the amplitude of the external field. This indicates that the reversal area in the Co film is continuously changing with field amplitude, i.e., the reversal proceeds via many magnetization jumps. (ii) The curve EF remains horizontal for each loop, which indicates that the characteristics of the domain structure (e.g., size, type of wall) does not change with decreasing field for each loop measurement, as is typical of domain-wall pinning. The reversal mechanism is therefore likely to be controlled by 180° domain-wall motion. If there is a switch from a 180° wall to a 90° wall with decreasing field (in a given loop) the curve EF would not be horizontal. However, a question that arises is whether 90° domains nucleate at low field amplitudes. Our following analysis will show that no such process occurs.

Consider a small area of Co layer including a 180° domain with the FeNi layer saturated as shown in Fig. 5(b). The measured resistance R represented by curve EF can be expressed as

$$R=(1-\sqrt{k})R_{\uparrow\downarrow}+\frac{\sqrt{k}R_{\uparrow\uparrow}R_{\uparrow\downarrow}}{R_{\uparrow\uparrow}+\sqrt{k}(R_{\uparrow\downarrow}-R_{\uparrow\uparrow})}, \qquad (2)$$

where k is the reversal fraction. As $k\to0$, $R=R_{\uparrow\downarrow}$, and as $k\to1$, $R=R_{\uparrow\uparrow}$. Using Eq. (2) and our experimental values of R obtained under different field amplitudes, we can obtain a relationship between the reversal fraction k and field amplitude (Fig. 6, curve 1). From the longitudinal MOKE measurement one can obtain a similar relationship (curve 2). For curve 2, k is obtained using $k=(I^S_{Py}/I_{Py})I_{Co}$, where I_{Co} is the height of the Co switch on the normalized loop measured
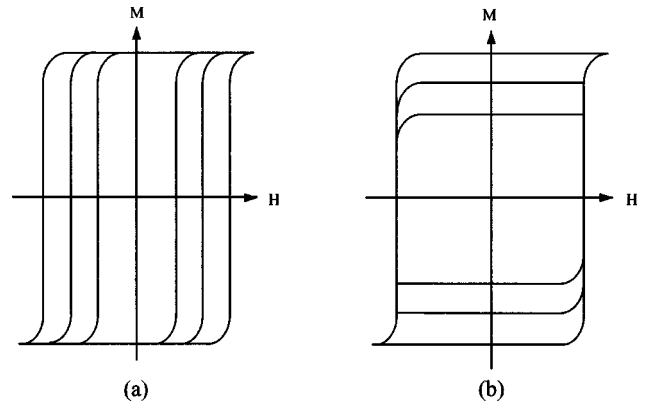
at a given field amplitude. I^S_{Py} and I_{Py} are the height of the FeNi switch on normalized loop measured under saturation and arbitrary field, respectively. The two curves coincide with each other very well, indicating that the assumption of reversal occurring by 180° domain-wall motion is correct.

C. Domain-wall pinning by interface roughness

Either domain nucleation or wall pinning can control the reversal mechanism of the Co film. The dominant mechanism can be evaluated from the evolution of the hysteresis loops with increasing field amplitude. For the nucleation mechanism the coercivity increases with external field amplitude [Fig. 7(a)], while for the wall-pinning mechanism the coercivity does not change with external field as shown schematically in Fig. 7(b).[12] In our case the MOKE loop evolves with external field, approximately as in the latter case (see Fig. 3), indicating domain-wall pinning, even though there is a slight increase in coercivity with field. .

The growth of a Co film on a Cu(001) surface has been shown to be almost layer-by-layer growth.[13] With such layer-by-layer growth the defects that pin the domain-wall motion are likely to be at the interface (both the bottom and top surface of the Co layer). For an ultrathin Co film, the Néel domain wall is so thin[14] ($\sim$50 Å) that a small defect can play an important role in the wall pinning. To verify this assumption we need to evaluate the size of the defect for

FIG. 7. Schematic of two kinds of hysteresis loops when the hysteresis behavior is controlled by (a) nucleation and (b) wall pinning.
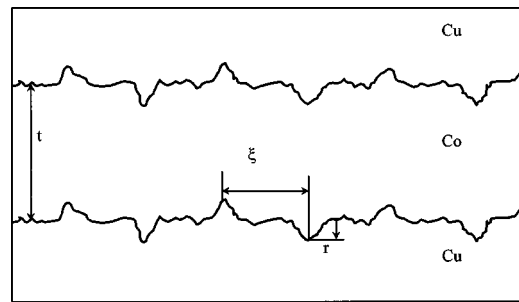

FIG. 8. A schematic of the roughness at the interfaces. Both bottom and top interfaces have the same roughness because of the layer-by-layer growth mechanism. There are small peaks and trenches with an average radius r and lateral distance ξ at the interfaces.

wall pinning and then compare with the interface roughness. We use a simple model of the surface structure (Fig. 8): On the bottom Cu layer there are small peaks and troughs with an average radius r and lateral distance ξ. Because of layer-by-layer growth the same roughness configuration is expected at the top Cu/Co interface. We will use Kersten's inclusion theory[15] because of its simplicity. This theory yields the following expression for the coercivity:

$$H_C = \frac{1.2 f^{2/3} E}{M_S r},\qquad(3)$$

where E is the domain-wall energy density, f is the volume fraction occupied by the inclusions, r is the radius of the inclusions, and M_S is the saturation magnetization of Co. Although in this model the inclusions are assumed to be large compared with the domain-wall width, for very small defects it can still apply.[16] For the ultrathin Co film the domain wall is of Néel type and its total wall energy density is expressed by adding the exchange, anisotropy, and magnetostatic contributions:

$$E = A\left(\frac{\pi}{\delta}\right)^2 \delta + \tfrac{1}{2}\delta k + \left(\frac{\pi\delta t}{\delta+t}\right)M_S^2,\qquad(4)$$

where A is an exchange stiffness, δ is the wall width, K is the anisotropy constant, and t is the film thickness. For fcc Co (Ref. 11) $A = 1.3\times10^{-6}$ erg/cm, $K = 6.3\times10^5$ erg/cm^3, M_S(fcc)$= M_S$(hcp)$=1431$ emu/cm^3. Neglecting both the exchange and anisotropy contribution, we obtain

$$H_C = \frac{1.2\pi f^{2/3}\delta t M_S}{r(\delta+t)}.\qquad(5)$$

From the roughness model shown in Fig. 8, we obtain the volume fraction $f=4\pi r^3/3\xi^2 t$, and substituting into Eq. (5) gives

$$H_C = \frac{9.8\delta r M_S t^{1/3}}{(\delta+t)\xi^{4/3}}.\qquad(6)$$

For our Co film $t\sim40$ Å, $\delta\sim50$ Å, $H_C\sim100$ Oe, and we can take $\xi\sim100$ Å as the lateral correlation length in the Co/Cu system.[14] Hence we obtain the value of r as ~1 Å, which is in agreement with the experimental value of the interface width in fcc Co/Cu.[14] The magnetization jumps in the M-H loop can be explained by the variation in the value of r associated with the interface structure.

If $t\ll\delta$, then Eq. (6) becomes

$$H_C = \frac{9.8 r M_S}{\xi^{4/3}} t^{1/3}.\qquad(7)$$

The thickness dependence of H_C is dependent on the system under consideration, for instance,[16] $H_C\sim t$ in Fe. The thickness dependence of H_C described in Eq. (7) is very weak ($\sim t^{1/3}$), and it can therefore explain why the coercivity of ultrathin Co/Cu(001) shows little variation with thickness.[14] Although the interface roughness plays an important role in the 180° wall pinning, it does not exclude other mechanisms such as bulk defects and grain boundaries.

IV. CONCLUSION

We have studied the magnetic domain configuration and magnetization-reversal processes in a ferromagnetic fcc cobalt film, with in-plane anisotropy, by GMR and MOKE methods. In the Cu/Co(40 Å)/Cu(001) film studied, 90° domain boundaries strongly dominate over 180° walls in the demagnetized state, but the magnetization-reversal process is controlled by 180° domain-wall motion. The 180° walls are found to undergo multiple jumps mainly due to domain-wall pinning associated with interface roughness.

*Electronic address: jacb1@phy.cam.ac.uk

[1] J. Ferré, V. Grolier, P. Meyer, S. Lemerle, A. Maziewski, E. Stefanowicz, S. V. Tarasenko, V. V. Tarasenko, M. Kisielewski, and D. Renard, Phys. Rev. B **55**, 15 092 (1997).

[2] Gabriel Bochi, H. J. Hug, D. I. Paul, B. Stiefel, A. Moser, I. Parashikov, H.-J. Güntherodt, and R. C. O'Handley, Phys. Rev. Lett. **75**, 1839 (1995).

[3] V. S. Gornakov, V. I. Nikitenko, L. H. Bennett, H. J. Brown, M. J. Donahue, W. F. Egelhoff, R. D. McMichael, and A. J. Shapiro, J. Appl. Phys. **81**, 5215 (1997).

[4] J. Urguris, R. J. Celotta, and D. T. Pierce, Phys. Rev. Lett. **69**, 1125 (1992).

[5] L. J. Heyderman, J. N. Chapman, and S. S. P. Parkin, J. Magn. Magn. Mater. **138**, 344 (1994).

[6] M. Rührig, R. Schäfer, A. Hubert, R. Mosler, J. A. Wolf, S. Demokritov, and P. Grundberg, Phys. Status Solidi A **125**, 635 (1991).

[7] U. Hartmann, J. Magn. Magn. Mater. **157-158**, 545 (1996).

[8] M. S. Valera, A. N. Farley, S. R. Hoon, L. Zhou, S. McVitie, and J. N. Chapman, Appl. Phys. Lett. **67**, 2566 (1995).

[9] A. Samad, B.-Ch. Choi, and J. A. C. Bland, Phys. Rev. B **60**, 7304 (1999).

[10] R. Allenspach, M. Stampanoni, and A. Bischof, Phys. Rev. Lett. **65**, 3344 (1990).

[11] H. P. Oepen, M. Benning, H. Ibach, C. M. Schneider, and J. Kirschner, J. Magn. Magn. Mater. **86**, L137 (1990).

[12] W. Zhong, *Ferromagnetics* (Scientific and Technological Press, Beijing, 1987), p. 356.

[13] B. Heinrich, J. F. Cochran, M. Kowalewski, J. Kirschner, Z. Celinski, A. S. Arrott, and K. Myrtle, Phys. Rev. B **44**, 9348 (1991).

[14] Q. Jiang, H.-N. Yang, and G.-C. Wang, Surf. Sci. **373**, 181 (1997).

[15] M. Kersten, *Grundlagen einer Theorie der Ferromagnetischen Hysterese und der Koerzitwkraft* (Hirzel, Leipzig, 1943).

[16] Y. K. Kim and M. Oliveria, J. Appl. Phys. **74**, 1233 (1993).